DEBRIS SELECTION AND OPTIMAL PATH PLANNING FOR DEBRIS REMOVAL ON THE SSO: IMPULSIVE-THRUST OPTION

J. T. Olympio and N. Frouvelle

CS-SI, 31506 Toulouse, France, Email: {joris.olympio, nicolas.frouvelle}@c-s.fr

ABSTRACT

The current paper deals with the mission design of a generic active space debris removal spacecraft. Considered debris are all on a sun-synchronous orbit. A perturbed Lambert's problem, modelling the transfer between two debris, is devised to take into account J2 perturbation, and to quickly evaluate mission scenarios. A robust approach, using techniques of global optimisation, is followed to find optimal debris sequence and mission strategy. Manoeuvres optimization is then performed to refine the selected trajectory scenarii.

Key words: Active Debris Removal; Maneuver Optimisation; SSO; Pertubed Dynamics.

1. INTRODUCTION

For the past decades, technological advances and customer needs have resulted in an increase of the space assets in space. However, current mandatory space debris mitigation policies are not sufficient to prevent the congestion of some orbits. The risk of in-orbit collisions between existing debris, or with active spacecraft, increases and this eventually results in new debris[8]. Latest debris population simulations show that even with no new launch, the debris population would increase[11]. This is because of a collisional cascading effect, known as the Kessler syndrome[8]. The Kessler Syndrome describes the phenomenon that the number of debris generated by random collisions between catalogued objects and debris is greater than the number of debris generated by collisions between catalogued objects and the natural meteoroid environment. The phenomenon is eventually the most important long-term source of debris because of the increase of the collision frequency with debris accumulation rates.

The space debris environment is indeed dynamic and versatile. The dynamics include several phenomenons such as the Earth's gravitational field and its harmonics, or the atmospheric drag. Eventually, the average growth rate of catalogued debris over the past 50 years has been about 300 objects per year because of the implementation of the IADC guidelines, natural effects, and political and economical situations[8].

Therefore, to limit the effect of the Kessler syndrome, the number of large non-cooperative objects (e.g., non-operational payloads, upper stage rocket bodies, broken spacecraft) in Earth orbit should be significantly reduced. In the order of 5 to 10 debris should be removed each year to stabilize the debris population[3]. Recently, a considerable amount of studies have been conducted to analyse or to devise different alternatives to remove debris such as: tethers or solar sails, robotic arms, foams, retro-electric propulsion, laser, nets and many more. All those concepts (except for lasers) require guiding an ADR platform to one debris, or many in sequence. Actual transfer cost with computation of the manoeuvres and trajectories is required to assess and refine the definition of any ADR platform.

The current paper focuses on the selection of debris to remove on sun-synchronous orbits (SSO) and, the guidance to the selected debris using chemical propulsion. The precise guidance in close proximity to the debris is not considered (discussion can be found in Ref. [2]), as well as the operations that have to be followed to remove the debris. Several criteria are used to select a list of debris to remove. A general approach is followed to find the best scenarii, with the dynamics including gravitational perturbations. The scenarii are refined using techniques of optimal control theory for impulsive transfers. The approach is applied to a set of about 900 debris in the SSO.

2. PROBLEM STATEMENT

2.1. Context and Assumptions

Debris to remove are either the biggest ones or those on the most crowded orbital regions. On the one hand, heavy debris have the potential of creating many more debris. On the other hand, debris on the most crowded orbital regimes, or those with high area, have the highest impact probability. Currently, the most crowded orbital regions are defined with,

- inclination in $[95, 100]$, $[70, 75]$ or $[80, 85]$, and

Proc. '6th European Conference on Space Debris'
Darmstadt, Germany, 22–25 April 2013 (ESA SP-723, August 2013)

- semi-major axis in $[800, 850]$ km, $[950, 1000]$ km, or $[1450, 1500]$ km

It has been suggested in recent papers that 5 to 10 debris should be removed every year for the Kessler syndrome to be controlled[8] [3]. We are interested in a multi-debris removal mission.

The following points are assumed:

1. The orbit determination problem is solved accurately from sufficient time in advance,
2. A given fixed time of close operation: rendezvous with the debris, attitude manoeuvres, and removal operation,
3. Autonomous navigation of the chaser spacecraft: all necessary information about the debris to remove are available,
4. A constant mass drop out is considered after each removal operation,
5. The chaser does not create new debris.

2.2. Transfer Strategy and Closing Phases

The mission scenario is defined with a debris sequence, and debris rendezvous dates. At the beginning of each mission, the satellite (chaser) is released by the launcher for a free transfer and rendezvous with the first debris (target).

Before final rendezvous with the target, the chaser has to perform a series of small manoeuvres to refine the orbit determination and to prepare the capture of the target. After the rendezvous, a de-orbit manoeuvre is performed to place the target on a reentry orbit such that the target orbital lifetime is sufficiently reduced. This phase is modelled a time duration $T^{de-orbit}$ accounting for the rendezvous phase and the de-orbitation manoeuvre operations.

Immediately after the de-orbitation manoeuvre, a mass drop on the chaser, independent of the debris features, is assumed. This mass loss can be attributed to the fuel necessary to perform the autonomous rendezvous, the proximity operations, the capture or the deployment and attachment of a subsystem on-board the target debris and, the de-orbitation manoeuvre.

In addition, after the de-orbitation manoeuvre, the chaser drifts on the orbit of the target during a waiting time T^{wait}. This time is variable and accounts for contingency plans, target reentry orbit observation and prediction and, optimal phasing for the transfer to the next target. Once the target orbital lifetime has been confirmed, and at the end of T^{wait}, the chaser can start a new transfer toward the next debris in the mission scenario, and so on. The mission is illustrated in the scheme of figure (1).

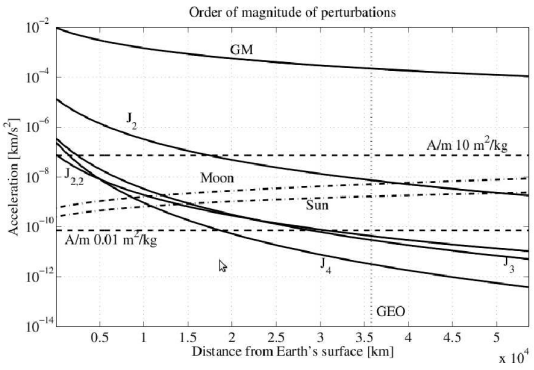

Figure 2. Order of magnitude of the perturbations in an orbit around Earth[7].

2.3. Dynamical Model

Debris dynamics are usually defined with a set of Two-Line Elements (TLE) and a propagator SGP4[13]. This simplified model allows predicting an orbital segment subject to perturbations such as drag, solar radiation, Earth's gravitational potential and other planetary gravitational effects. However, debris ephemerides accuracy degrades with time, and the TLE information have to be updated regularly. Besides, information about rotational rate of debris, or their physical characteristics having an influence on dynamics are not always available. In the current paper, it is assumed that the debris state is known perfectly.

Figure 2 compares the influence of the drag force, and several gravitational perturbations from the Moon and the Sun, and the Earth gravitational field harmonics zonal terms J_2, J_3 and J_4, for instance. The three main contributions to the dynamics are the central body gravity field harmonics (related to J_0 and J_2, and the atmospheric drag.

For debris in the SSO (around 800-900km) the altitude is high enough for atmospheric density to be small and the drag to be considered a negligible factor to the short-term orbital evolution. The potential owing to the J_2 contribution in the gravitational field of Earth is[4],

$$R = -\frac{\mu J_2 r_{eq}^2}{2p^3}\left(1+e\cos f\right)^3\left(3\sin^2\left(w+f\right)\sin^2 i - 1\right) \tag{1}$$

where i is the current orbit inclination with respect to the equatorial plane, e is the orbit eccentricity, ω the argument of perigee, f the true anomaly, and p the orbit parameter. Accounting for the J_2 effect alone, the average

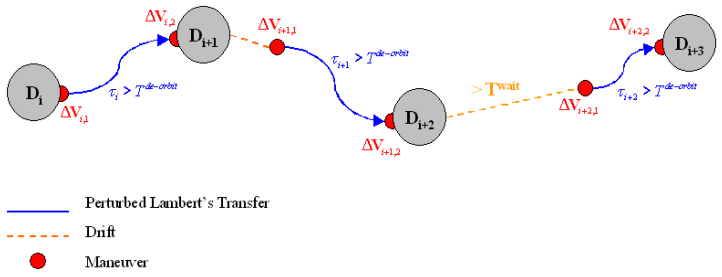

Figure 1. Scheme of the transfer sequence.

secular variations on the orbital elements is,

$$\overline{\frac{d\omega}{dt}} = J_0 n_0 \frac{5\cos^2 i - 1}{2p^2} \tag{2}$$

$$\overline{\frac{d\Omega}{dt}} = -J_0 n_0 \frac{\cos i}{p^2} \tag{3}$$

$$\overline{\frac{dM}{dt}} = n_0 \left(1 + J_0 \sqrt{1-e^2}(3\cos^2 i - 1)\right) \tag{4}$$

where

$$J_0 = \frac{3}{2}\mu J_2 r_{eq}^2$$

and, Ω stands for the longitude of ascending node (RAAN). The unperturbed mean motion is denoted n_0 while the mean motion taking into accounts secular variations is denoted n. Eventually, the dynamical equation in Cartesian coordinates is,

$$\frac{d^2\mathbf{r}}{dt} = \mathbf{f}_0(\mathbf{r}) = -\mu\frac{\mathbf{r}}{r^3} - \frac{J_0}{r^5}\left[\left(1 - 5\frac{z^2}{r^2}\right)\mathbf{r} + 2z\mathbf{u}_z\right] \tag{5}$$

where $\mathbf{r}$ is the position vector in a Earth centred frame, $\mathbf{u}_z$ is the unit vector normal to the equatorial plane, and $z = \mathbf{r}^T\mathbf{u}_z$.

This demonstrates that orbits in the SSO regime will tend to drift slightly with time (mainly for the longitude of ascending node). The secular effect of both Ω and ω will tend to increase with the inclination and the eccentricity. It is important to note that the average change per orbit of a, e and i is null, but these quantities still change slightly over one revolution.

2.4. Transfer model: Lambert's Problem with Earth Oblateness Perturbation

The transfer from debris D_i to debris $D_j \neq D_i$ is computed using a perturbed Lambert's problem solver. The original unperturbed Lambert's problem is the problem of finding the arc of conic, using Gibbs' theorem, of a given duration $t_j - t_i$, solving a two-points boundary value problem[4]. The solution gives the osculating orbital parameters at departure time t_i that leads to the orbital position of D_j at final time t_j under perturbed Keplerian dynamics (see eq. 5). The initial $\Delta\mathbf{V}_i$[1] and final $\Delta\mathbf{V}_j$, hence a transfer cost $\Delta V^{i,j} = \Delta V_i + \Delta V_j$, can be evaluated.

As was depicted in the section 2.3, depending on the orbital regime the dynamics can be prone to secular effects. Therefore, the original unperturbed Lambert's problem solvers is ill-suited for Earth-bound transfers between objects in the SSO.

However, it is possible to model J_2 perturbation effectively, and devise a pertubed Lambert's problem solver. Given the general dynamics described by Eq. (5), consider successive change of variables (Sundman transformation, KS transformation):

$$dt = rds \quad \mathbf{r} = \mathbf{L}(\mathbf{u})\mathbf{u}$$

The dynamical equations become

$$\ddot{\mathbf{u}} + \epsilon\mathbf{u} = \mathbf{Q}(\mathbf{u})$$

where ϵ represents a normalized energy, and $\mathbf{Q}$ is the perturbation term in the KS space. It is important to note that this ordinary differential equation is the one of an oscillator. Using classical results of calculus, the solution is the combination of the homogeneous solution (solution without the right hand part) and a particular solution. The homogeneous solution is obviously the solution with no perturbation, and the particular solution can be computed analytically using variation of parameters to account for the perturbation terms. The unperturbed Lambert's problem can then be adapted to the perturbed dynamics[6]. Using this approach, we have a fast and fairly accurate Lambert's problem solver able to quicly evaluate a transfer between debris.

Table 1 compares the different method and implementation for J2-perturbed Lambert's problem solvers. Several cases are presented. For each case, the initial velocity $\mathbf{V}_0$ and position $\mathbf{R}_0$ are propagated during T with a J_2 model providing a final position $\mathbf{R}_f$ and velocity $\mathbf{V}_f$. Then, the Lambert's problem is solved between $\mathbf{R}_0$ and $\mathbf{R}_f$, with a time of flight T, for each method (unperturbed, perturbed). The reference is given by a numerical, which consists on numerical integration and on using a state transition matrix to find the initial velocity $\mathbf{V}_0$ for the final position vector $\mathbf{R}(T)$ to match $\mathbf{R}_f$.

[1] $\Delta\mathbf{V}_i$ is the immediate change of velocity at time t_i: $\Delta\mathbf{V}_i = \mathbf{v}(t_i^+) - \mathbf{v}(t_i^-)$, and $\Delta V_i = \|\Delta\mathbf{V}_i\|$

Table 1. Comparison of perturbed Lambert's problem methods. Case 1 : $R_0 = [6478, 0, 0]km$, $R_f = [10970.928, 1435.480, 4304.951]km$, and $T = 1800.0009s$[6]. Case 2: same object on a SSO at two different epochs, $T = 1800s$. case 3: Case 2 with 1 revolution and $T = 10000s$. Case 4: case 2 with 2 revolutions and $T = 20000s$. case 5: Case 2 with 10 revolutions and $T = 60000s$. $\epsilon_{\mathbf{V}_0}$ and $\epsilon_{\mathbf{V}_f}$ are the error in velocity for $\mathbf{V}_0$ and $\mathbf{V}_f$, respectively.

Case	Method	Initial velocity $\mathbf{V}_0$, m/s	Final Velocity $\mathbf{V}_f$, m/s	$\lvert\epsilon_{\mathbf{V}_0}\rvert, \lvert\epsilon_{\mathbf{V}_f}\rvert$ m/s
1	Reference	7000.0 1000.0 3000.0	-444.7 532.3 1595.3	-
	Unperturbed	6996.6 999.9 2998.7	-443.8 532.4 1596.5	3.6, 1.4
	Perturbed-Lambert	7000.0 1000.0 3000.0	-446.3 532.1 1594.3	0.0, 0.3
2	Reference	700.9 2181.9 7063.3	-6988.9 1631.9 -2110.4	-
	Unperturbed	702.6 2184.7 7058.9	-6994.4 1625.7 -2113.4	5.3, 8.8
	Perturbed-Lambert	700.9 2181.9 7063.3	-6988.9 1632.0 -2110.1	0.2, 0.3
3	Reference	-679.2 2828.9 7611.5	-7806.3 2336.3 -905.1	-
	Unperturbed	-674.4 2835.4 7606.7	-7817.1 2316.6 -905.0	9.3, 22.6
	Perturbed-Lambert	-679.2 2828.9 7611.5	-7806.4 2336.6 -904.5	0.1, 0.2
4	Reference	-912.6 2936.0 7707.6	-7943.4 2466.0 -705.2	-
	Unperturbed	-904.3 2945.4 7702.2	-7958.5 2433.0 -704.1	13.8, 36.3
	Perturbed-Lambert	-912.9 2936.0 7707.6	-7943.5 2466.2 -705.1	0.1, 0.2
5	Reference	978.5 1995.1 6972.4	-6762.7 1657.7 -2427.0	-
	Unperturbed	981.5 2054.7 6953.0	-6832.9 1487.2 -2359.1	62.7, 199.9
	Perturbed-Lambert	975.4 1995.4 6974.0	-6762.9 1661.9 -2426.4	3.5, 4.3

3. GLOBAL SEARCH OF DEBRIS REMOVAL SCENARII

3.1. Search Space

Let's note D the set of debris. It is now possible to evaluate complete scenarii using the perturbed Lambert's problem solver. On a side note, this approach has been often followed for interplanetary mission analysis (e.g., asteroid tour). The main transfer parameter is the number of revolutions. In the multiple revolution Lambert's problem, there exists a minimum time of flight for each number of revolutions. Noting $\Omega_i(t_i)$ and $\Omega_j(t_i)$, the longitude of ascending node of the departing debris d_i and target debris d_j respectively, the following heuristic is used:

$$T_{rev} = \frac{|\Omega_j(t_i) - \Omega_i(t_i)|}{\bar{\dot{\Omega}}} \tag{6}$$

$$T_{min}^{i,j} = N_{rev} T_{per} \tag{7}$$

where $\bar{\dot{\Omega}}$ is a parameter defining an average rate of change of the longitude of ascending node, and T_{per} is an average period time. When seeking a transfer between d_i and d_j, all solutions that have a time of flight $T < T_{min}^{i,j}$ would have high orbital energy, and important phasing manoeuvres are expected. If inclination of both debris' orbits is the same, then N_{rev} defines exactly the number of revolutions necessary for a free correction of the longitude of ascending node when on an intermediate orbit having a secular variation of the longitude of ascending node equals to $\bar{\dot{\Omega}}$.

The decision vector that describes uniquely a transfer I is then $\mathbf{X}^I = [d_0^I, d_f^I, T^{0,I}, \tau^I]$, where $d_0^I \in D$ and $d_f^I \in D$ are respectively the initial and final debris, $T^{0,I}$ is the departure date from debris d_0^I, and $\tau^I > T^{de-orbit}$ is the transfer time from debris d_0^I to rendezvous with debris d_f^I. The date of arrival at debris d_f^I is denoted $T^{f,I} = T^{0,I} + \tau^I$.

3.2. Branch and Bound Method for Debris Selection

The branch and bound method consists in enumerating all possible solutions of a combinatorial optimisation problem. In the current paper, it is mainly used to find the debris sequence. A global search is made on a multi-dimensional grid $D \times D \times T \times \tau$ (the dimension is the one of the decision vector). Methods of global optimisation are well suited for problems with large dimensional space. The objective of those methods is to find the globally best solution, however, those techniques tends to find a neighborhood of the best solution rapidly rather than accurately. Therefore, they are usually used to get a good initial guess. This initial guess is then used with local optimisation techniques to get a refined, accurate, solution. This approach is followed in the current paper.

3.2.1. Objective function

The main purpose of the mission is to remove mass in orbits. The mass of space debris to remove should be maximized, and likewise to many space missions, the fuel requirement (total ΔV cost) should be minimized. Both output should be included in the objective function. It is also important to assess the impact the removing of a debris has on the environment. Generally, this can only be considered when using expensive debris population simulators. More simply, in addition to the debris mass m_i,

the debris area A_i should be considered because it influences the probability of collision. Therefore, the objective function should be constructed with a combination of those criteria, such as

$$J_i = \alpha \Delta V_i + \beta m_i + \gamma A_i \tag{8}$$

$$J = \sum_{i \in D} J_i \tag{9}$$

where α, β, γ are weighting factors. Typically, α would be in s/m, β in $1/kg$, and γ in $1/m^2$. The weighting factors have to be adjusted according to exact context of the mission.

3.2.2. Grid Search

To find the most interesting transfer features, a grid search with space pruning is used because it has the advantage of providing an exhaustive search. Each debris-to-debris transfer I depends only on the position and velocity vectors of the initial and final debris, $d^{0,I}$ and $d^{f,I} \in D \setminus \{d^{0,I}\}$, at the initial and final dates $T^{0,I}$ and $T^{f,I}$ respectively. Therefore, each transfer I can be computed separately, without knowledge of the previous transfers, for all initial and final dates, which makes the global search parallelisable. The debris-to-debris transfers can then be evaluated using Graphical Processing Units (GPU), or other parallel architecture, to solve the multiple perturbed Lambert's problems (sec. 2.4), with limited computational time[1].

Once every possible transfers have been computed, complete scenarios can be constructed, in a branch and bounds manner, patching together the transfer segments I and J according to their initial and final dates ($T^{0,J} - T^{f,I} > T^{wait}$) if debris at the junction are the same ($d^{f,I} = d^{0,I'}$). The total cost of the constructed debris sequences can then be evaluated.

3.2.3. Search Space Pruning

Pruning constraints are used to speed-up overall process by reducing the search space. These constraints should not prevent finding good solutions, but rather quickly discard the parts of the search space where good solutions are unlikely to exist. Any rendezvous transfers can be executed using an inclination change manoeuvre ΔV^{inc}, an altitude change manoeuvre ΔV^{Hoh}) and, a phasing correction manoeuvre Δ_V^{ϕ}. ΔV^{inc} and ΔV^{Hoh} are very fast to compute, in contrast with the computation of Δ_V^{ϕ} (it requires solving the Lambert's problem). Therefore, the pruning constraint is $\Delta V^{inc} + \Delta V^{Hoh}$. If it is above a given threshold ΔV^{max}, the debris transfer branch is discarded, and so part of the search space removed. Otherwise, the transfer is computed solving the perturbed Lambert's problem.

4. OPTIMAL GUIDANCE BETWEEN DEBRIS: IMPULSIVE PROBLEM

In this section, the state of the spacecraft is denoted $\mathbf{x} = [\mathbf{r}; \mathbf{v}; m]$, where $\mathbf{r}$ and $\mathbf{v}$ are respectively the position and velocity vector in an Earth centred inertial frame, and m is the spacecraft's mass. At rendezvous with a debris I at date t_I, the position and velocity vectors of the spacecraft match, respectively, the position and velocity of that debris: $\mathbf{r}(t_I) = \mathbf{r}_I(t_I)$ and $\mathbf{v}(t_I) = \mathbf{v}_I(t_I)$. We assume that the global optimisation successfully return a scenario (debris sequence and rendezvous dates) minimizing the cost defined in Eq. (9). The purpose of the optimal guidance is now to improve the solution by finding an optimal sequence of manoeuvres that minimizes the required propellant mass for the mission.

4.1. Problem Formulation

The guidance for a spacecraft equipped with a chemical propulsion system is composed of short burn arcs. They are generally modelled as impulses since the burn arc duration is small compared to the mission duration. With this infinite impulse model, the dynamics do not depend on the mass. But, the mass can be computed using Toltoiskii formula,

$$\Delta V = \sum_i \Delta V_i = g_0 I_{sp} \ln \left(\frac{m(t_0)}{m(t_f)} \right) \tag{10}$$

where $m(t_0)$ and $m(t_f)$ are the initial and final mass respectively, I_{sp} is the specific impulse defining the efficiency of the chemical propulsion system. The performance of the mission is measured in terms of total ΔV, the optimal control problem is to minimize it. Since the problem is defined with rendezvous and departure maneuver constraints, and the mass is not taken into account for impulsive trajectories, the influence of one phase (debris-to-debris segment) over an other is negligible. Optimizing the entire mission of N phases is then equivalent to solving N independent optimisation sub-problems.

Each impulse i is described by a date t_i and an impulse vector $\Delta \mathbf{V}_i$ (many other models are possible). Therefore, the transfer from debris I to debris J (different of I) is given by the sub-problem,

$$\min_{t_i, \mathbf{r}_i} \sum_i \Delta V_i \tag{11}$$

$$\text{s.t.} \quad \frac{d^2\mathbf{r}}{dt^2} = \mathbf{f}_0(\mathbf{x}; t) \tag{12}$$

$$\Delta V_i = \left\| \mathbf{v}(t_i^+) - \mathbf{v}(t_i^-) \right\| \tag{13}$$

$$\boldsymbol{\psi}(t_i) = \mathbf{r}(t_i^+) - \mathbf{r}(t_i^-) \tag{14}$$

The intermediate constraints $\boldsymbol{\psi}(t_i)$ ensure the position continuity across impulses. Obviously, it is not necessary to use a Lambert's problem solver (in which case

constraint $\psi(t_i)$ would be implicitly satisfied), but one can also simply integrate the exact dynamics, eq. (5), between impulses.

4.2. Optimal Control

The number of impulses are determined using the primer vector theory[9][10][12] adapted to the current perturbed dynamics. The date and amplitude of each impulse is found using a non-linear solver, while the primer vector theory provides also an initial guess for the date. Even though experience dictates that impulses be placed near apogees and perigees, primer vector theory gives an exact framework for optimisation, and in particular for the considered perturbed dynamics.

To construct the primer vector $\|\boldsymbol{\lambda}_\mathbf{v}\|$ history, consider

$$\frac{d^2\boldsymbol{\lambda}_\mathbf{v}}{dt^2} = \mathbf{G}(\mathbf{r};t)\boldsymbol{\lambda}_\mathbf{v} \tag{15}$$

with boundary conditions,

$$\boldsymbol{\lambda}_\mathbf{v}(t_0) = \frac{\Delta\mathbf{V}_0}{\|\Delta\mathbf{V}_0\|}, \qquad \boldsymbol{\lambda}_\mathbf{v}(t_f) = \frac{\Delta\mathbf{V}_f}{\|\Delta\mathbf{V}_f\|} \tag{16}$$

The gravity gradient matrix $\mathbf{G} = \mathbf{G}_{kep} + \mathbf{G}_{pert}$ is given by,

$$\mathbf{G}_{kep} = \mu\left(\frac{\mathbf{I}_{3,3}}{r^3} - 3\frac{\mathbf{r}\mathbf{r}'}{r^5}\right)$$
$$\mathbf{G}_{pert} = -J_0\frac{\partial}{\partial\mathbf{r}}\left\{\frac{1}{r^5}\left[\left(1-5\frac{z^2}{r^2}\right)\mathbf{r} + 2z\mathbf{u}_z\right]\right\}$$

Similarly to switching functions, the amplitude of $\|\boldsymbol{\lambda}_\mathbf{v}\|$ gives the time location of optimal impulses. A trajectory with impulses is then optimal when at each impulse $\|\boldsymbol{\lambda}_\mathbf{v}\| = 1$, and $\|\boldsymbol{\lambda}_\mathbf{v}\| < 1$ elsewhere. If $\|\boldsymbol{\lambda}_\mathbf{v}\| > 1$ on a given time interval, an impulse should be added in that region, or the current manoeuvre strategy modified.

An iterative process is put in place to solve the problem. From an initial guess, the amplitude of $\|\boldsymbol{\lambda}\|(t)$ is computed and optimality of the solution checked. Impulses are added if necessary, and optimized with a non-linear optimizer. Upon convergence of the optimizer, the process is restarted, first checking for the optimality of the solution and then adding new manoeuvres if necessary, and so on. An algorithm can be found in Ref. [12]. For best accuracy, the gradient of the objective function, and the Jacobian of the constraints are computed numerically using transition matrices. The initial guess is the initial transfer trajectory with the predicted manoeuvres assigned with a zero amplitude (using the perturbed problem rather than averaged equations is then of significance).

5. APPLICATION

5.1. Definition of the Mission

The vehicle is assumed a 20-ton spacecraft with complete systems for autonomous rendezvous, such as vision based guidance, radar, lidar, and GPS. A well qualified removal system is assumed. Because of the strong gravity field, and to accommodate reasonable transfer time between space debris, the spacecraft uses solar electric propulsion with 0.5 N and 2500 s specific impulse.

5.2. Selection of the Targets

5.2.1. Debris Population Definition

Figure 3 depicts the space debris densities for different orbital regimes, where data were extracted from Celestrak. The most crowded region is the one with altitude 800 km, and inclination 82 degrees. Figure 4 shows the randomly generated debris set. The mass of each debris was generated randomly with normal distribution.

5.2.2. Pruning Values for the Global Search

Section 3 helps finding a sequence of debris using no DSM. Impulses were only applied when leaving or rendezvousing a debris. Thanks to the perturbed Lambert's problem, the coast dynamics allow free change of the longitude of ascending node; a set of low-cost debris scenario as been obtained under those conditions. Manoeuvres can be added to improve the solutions and reduced their ΔV. This manoeuvres can improve the cost quite substantially, and indeed the pruning threshold ΔV^{max} has to be chosen carefully: setting it large to keep potentially good solutions, but not too large to limit the amount of data to compute. The approximate ΔV to de-orbit an average debris of 1500 kg from the SSO with a one-burn transfer is $\Delta V \approx 220m/s$. Therefore, since fuel is spent either on a de-orbiting device, or on-board the chaser spacecraft, to de-orbit the debris, it is assumed a mass drop ΔM^{drop} corresponding to that ΔV (for an engine of specific impulse 315 s).

We choose for the global search, $\alpha = 1m^{-1}s$, $\beta = 2000kg^{-1}$ and $\gamma = 0m^{-2}$ (no information on surface were generated or collected for this study). The global search is defined with,

$$\begin{aligned} \Delta TOF &= 15\ min & TOF &\in [5\ min; 40hours] \\ \Delta T0 &= 30\ min & T0 &\in [7305; 7670]\ MJD2000 \\ T^{de-orbit} &= 5days & T^{wait} &= 2days \end{aligned}$$

This yields to a high computational complexity, which fortunately can be tackled efficiently in little time using GPU. The overall computational time is of the order of

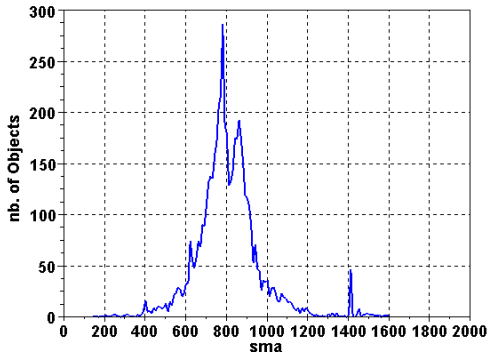

Figure 3. Space debris repartition on the different orbital altitudes.

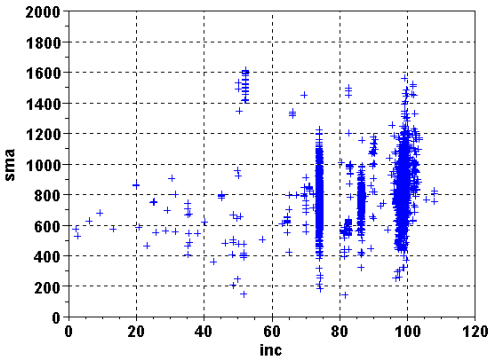

Figure 4. Debris population. Semi-major axis versus inclination.

few hours. There is no need to define a very fine grid, because at this stage we are looking for good debris sequences and, the solution will be refined with the local optimisation methods.

5.2.3. Results

Figure 5 depicts the cost of all computed debris-to-debris transfers. The ΔV cost starts from 5 m/s, which demonstrate very good phasing conditions, to 500 m/s, as a result of pruning constraints. Figure 6 shows the debris mass removed versus total ΔV. A trend can be observed on figure 6, as the more mass is removed, the more ΔV is required. However, some points seem to give a very high mass over delta-V ratio. Obviously, at this point, the ΔV have not been optimised. The mission has a duration limit of one year, but among all the feasible 5-debris-removed solutions obtained during the grid search, very few reach that limit. That shows that more than 5 debris can potentially be de-orbited.

Table 2 summarises the optimisation of two solution results of the global search. It illustrates the substantial improvement in cost after the manoeuvre optimisation. The reason of those gains comes mainly because solutions have many revolutions, and thus inserting intermediate maneuvers can drastically reduces the delta-V cost of the final maneuver. Furthermore, because of the numerical integration during the local optimisation, all possible defects owing to the analytical model used in the Lambert's problem vanish. Final results are thus accurate for the considered dynamical model (J2 only, no averaging).

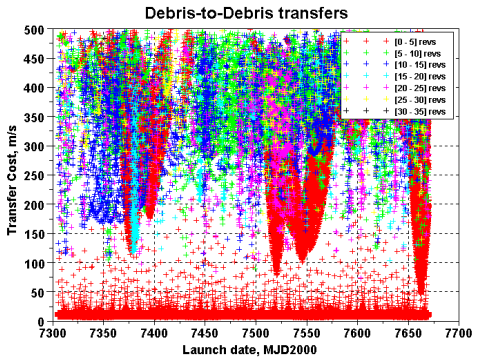

Figure 5. Set of debris-to-debris transfers.

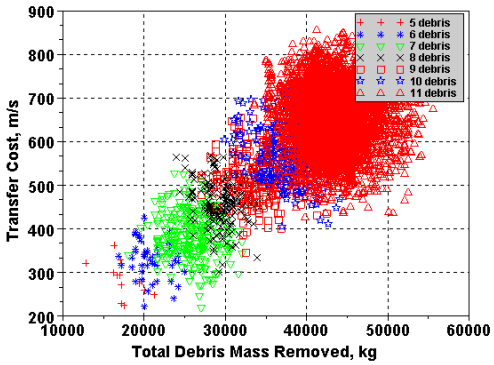

Figure 6. Feasible solutions of the grid search, mass versus ΔV.

The second point is that the ΔV are quite low (from 200 m/s to 861 m/s), but still of the same order of magnitude than the simulation of Ref. [5] for a different debris population of the same orbital regime. As we allowed the removal from 5 to 11 debris, indeed, almost all the most expensive transfers, around 800 m/s, refer to 11-debris removal scenario. But, the lowest transfer scenario have 6 or more debris. Most of the total time of flight consist in drifting phases for optimal phasing.

Solution	Leg Cost, m/s				Total	Nb.
	1	2	3	4	m/s	Impulses
Nominal 1	186.4	174.7	83.9	23.0	468.1	8
Optimal 1	165.1	80.0	31.8	21.6	298.5	135
Nominal 2	191.3	188.4	166.8	179.5	726.0	8
Optimal 2	154.9	101.8	61.1	46.5	264.4	134

Table 2. Optimisation of two transfers.

5.3. Conclusion

A perturbed transfer model has been used to quickly evaluate transfers between debris. A grid search was conducted to find the best debris-to-debris transfers, and subsenquently construct 5- to 10-debris sequences. It has been shown that for a reprensetative debris population, the cost of removing 5 debris per year can be below 500 m/s. Indeed, the natural dynamical perturbation can be used to phase naturally with debris, and several intermediate maneuvers can be found to lower the transfer cost.

Low-thrust transfers should provide very interesting alternative solutions, provided the thrust-levels are sufficient to respect the same time horizons.

REFERENCES

1. N. Arora and R.P. Russell. A gpu accelerated multiple revolution lambert solver for fast mission design. In *Advances in the Astronautical Sciences*, volume 136, 2010.
2. B.W. Barbee, J.R. Carpenter, S. Heatwole, F. Landis Markley, M. Moreau, Bo J. Naasz, and J. Van Eepoel. A guidance and navigation strategy for rendezvous and proximity operations with a noncooperative spacecraft in geosynchronous orbit. *The Journal of the Astronautical Sciences*, 58(3), May 2010. Special Issue: The George H. Born Astronautics Symposium.
3. B Bastida Virgili and H. Krag. Strategies for active removal in leo. In *5th European Conference on Space Debris*, 2009.
4. R.H. Battin. *An Introduction to the Mathematics and Methods of Astrodynamics*, chapter 3.6. AIAA Education Series. American Institute of Aeronautics and Astronautics, New York, revised edition, 1999.
5. Max Cerf. Multiple space debris collecting mission - debris selection and trajectory optimization. *Journal of Optimization Theory and Application*, 2012. doi:10.1007/s10957-012-0130-6.
6. R.C Engels and J.L. Junkins. The gravity-perturbed lambert problem: A ks variation of parameters approach. *Celestial mechanics and dynamical astronomy*, 24:3–21, 1981.
7. P. Fortescue, J. Stark, and G. Swinerd. *Spacecraft Systems Engineering*. John Wiley - Sons, March 2003.
8. D.J. Kessler, N.L. Johnson, J.-C. Liou, and M. Matney. The kessler syndrome: Implications to future space operations. In *33rd Annual AAS Guidance and Control Conference*, 2010. AAS 10-016.
9. D.F. Lawden. *Optimal Trajectories for Space Navigation*. Butterworths, London, 1963.
10. P.M Lion and M. Handelsman. Primer vector on fixed time impulsive trajectories. *AIAA Journal*, 6(1), 1968.
11. J.C. Liou and N.L. Johnson. Instability of the present leo satellite populations. *Advances in Space Research*, 41(7):1046–1053, 2008. doi:10.1016/j.asr.2007.04.081.
12. J. Olympio. Designing optimal multi-gravity-assist trajectories with free number of impulses. In *International Symposium on Space Flight Dynamics*, 2009.
13. Hoots F. R. and R. L. Roehrich. Spacetrack report no. 3: Models for propagation of norad element sets. Technical report, December 1980. Package Compiled by TS Kelso 31 December 1988.